UCRL-JRNL-215987

LAWRENCE
LIVERMORE
NATIONAL
LABORATORY

A Spectroscopic Comparison of Femtosecond Laser Modified Fused Silica using kHz and MHz Laser Systems.

W. J. Reichman, D. M. Krol, L. Shah, F. Yoshino, A. Arai, S. M. Eaton, P. R. Herman

October 6, 2005

Journal of Applied Physics

This document was prepared as an account of work sponsored by an agency of the United States Government. Neither the United States Government nor the University of California nor any of their employees, makes any warranty, express or implied, or assumes any legal liability or responsibility for the accuracy, completeness, or usefulness of any information, apparatus, product, or process disclosed, or represents that its use would not infringe privately owned rights. Reference herein to any specific commercial product, process, or service by trade name, trademark, manufacturer, or otherwise, does not necessarily constitute or imply its endorsement, recommendation, or favoring by the United States Government or the University of California. The views and opinions of authors expressed herein do not necessarily state or reflect those of the United States Government or the University of California, and shall not be used for advertising or product endorsement purposes.

Updated October 14, 2003

A Spectroscopic Comparison of Femtosecond Laser Modified Fused Silica using kHz and MHz Laser Systems.

Wilbur J. Reichman, Denise M. Krol,
Department of Applied Science, University of California, Davis, CA and
Lawrence Livermore National Lab, Livermore, CA, USA
Lawrence Shah, Fumiyo Yoshino, Alan Arai
IMRA America, Inc., Fremont, CA, USA
Shane M. Eaton, Peter R. Herman
Department of Electrical and Computer Engineering, University of Toronto,
Toronto, Ontario, Canada

ABSTRACT

Waveguides were written in fused silica using both a femtosecond fiber laser with a 1 MHz pulse repetition rate and a femtosecond amplified Ti:sapphire laser with a 1 kHz repetition rate. Confocal Raman and fluorescence microscopy were used to study structural changes in the waveguides written with both systems. A broad fluorescence band, centered at 650 nm, associated with non-bridging oxygen hole center (NBOHC) defects was observed after waveguide fabrication with the MHz laser. With the kHz laser system these defects were only observed for pulse energies above 1 μJ. Far fewer NBOHC defects were formed with the MHz laser than with kHz writing, possibly due to thermal annealing driven by heat accumulation effects at 1 MHz. When the kHz laser was used with pulse energies below 1 μJ, the predominant fluorescence was centered at 550 nm, a band assigned to the presence of silicon clusters ($E_{\delta}^{'}$). We also observed an increase in the intensity of the 605 cm^{-1} Raman peak relative to the total Raman intensity, corresponding to an increase in the concentration of 3-membered rings in the lines fabricated with both laser systems.

1. Introduction

In the mid 90s, it was discovered that femtosecond (fs) laser pulses could induce a localized refractive index change in glasses [1]. This phenomenon drew immediate interest because of its potential for fabricating optical devices inside bulk materials, with possible applications involving telecommunications devices, chemical / biological sensors, and data storage. Various groups have since used this localized refractive index change to fabricate many optical devices including waveguides, splitters, couplers, and lasers [1-9].

Despite this success, the underlying mechanisms of how femtosecond laser pulses induce a refractive index change are not fully understood. This problem can be simplified by splitting it into two questions: How is the energy from the fs laser pulse absorbed? And, how does the energy dissipate?

The energy absorption process has been fairly well characterized by fs laser ablation studies [10-14] and it involves multi-photon ionization followed by avalanche ionization to create a plasma.

There is less certainty regarding the energy dissipation process. It is believed that the primary mechanisms are a combination of thermal diffusion and shock wave generation, but it is uncertain which process is dominant and how long the processes take. Thermal diffusion dissipates heat through conduction within the material [1]. Shock

wave generation may result from the plasma expanding rapidly, creating a pressure wave that travels through the material [15]. Both of these processes could lead to rapid cooling, or quenching of the modified region. While the exact process is uncertain, the end results are localized physical, chemical, and structural changes of the material exposed to the laser beam. These alterations can involve densification, refractive index changes, and/or color center formation.

Recently, several groups have reported a large dependence of the localized modification on the laser pulse repetition rate. Traditionally, kilohertz repetition rate, amplified fs lasers have been used for fs device fabrication because high-repetition rate oscillators have not had high enough pulse energies. However, the recent development of high power oscillators and other high repetition rate, fs sources has overcome this barrier. The principle differences reported when using high repetition rate lasers are an increase in the perceived line diameter due to thermal diffusion and heat accumulation [16-17], and a potentially greater refractive index modification [18]. Additionally, it has been observed that megahertz systems provide better quality waveguides in some transparent glasses, while kilohertz systems are favored by other materials. Currently, it is unknown why some materials respond better with one laser or the other.

In order to better understand the differences in how kilohertz and megahertz repetition rate laser systems modify transparent materials, we used Raman and fluorescence spectroscopy to compare fused silica modified by an amplified 1 kHz fs laser and a 1 MHz fs fiber laser. Previous work on waveguides written in fused silica

using a kilohertz repetition rate laser has shown that the intensities of the Raman peaks at 490 and 605 cm^{-1} relative to the total Raman intensity are much higher in the modified glass, indicating an enriched population of three- and four-membered ring structures [19–20]. This enrichment is consistent with a higher density, higher fictive temperature, and higher refractive index of the fused silica [21-24]. There is also an increase in fluorescence in the modified region with a peak around 650 nm due to the formation of non-bridging oxygen hole centers (NBOHC). Both features are known to increase with increased irradiance when using a kHz laser system.

2. Experiment

Waveguides were fabricated in fused silica (Corning 7940) using an amplified, 1 kilohertz, Ti:Sapphire femtosecond laser (Millennia-Tsunami oscillator in combination with a Merlin-Spitfire amplifier, all from Spectra Physics, Inc.) and a 1 megahertz, frequency-doubled Yb-fiber laser (FPCA μJewel from IMRA America, Inc.). The kilohertz laser was operated at 800 nm with 130 fs pulses, and 0 to 5 μJ pulse energies. It was focused into silica cubes using a 50X 0.55 NA objective, and the sample was moved either longitudinally or transversely to the direction of the laser beam at 20 μm/s. These conditions match the conditions reported earlier in references 19 and 20, so that the results are directly comparable. The megahertz laser was operated at 522 nm with ≤500fs pulses, using 90 and 115 nJ pulse energies. It was focused into silica plates using a 100X 0.85NA objective, and the sample was moved transversely at 0.05 to 5 mm/s. These were the conditions with the highest cumulative dose reported earlier [18].

A scanning confocal microscope was used to simultaneously collect Raman and fluorescence spectra of the sample. A 50 mW, 488 nm Argon ion laser was focused into the sample using a 100X 0.73 NA microscope objective. The backscattered Raman and back-emitted fluorescence were then collected using the same objective; and a 0.25 m spectrometer with a 300 groove mm^{-1} grating and a liquid nitrogen cooled CCD array detector, with a 5 minute acquisition time. Three spectra were collected from different points along the center of each waveguide. The spatial profiles of select waveguides were measured by scanning the sample with respect to the objective focus with a 1 μm step size traveling perpendicular to (across) the waveguides, and a 3 μm step size traveling along the waveguides. Fluorescence photobleaching was studied by continuously exposing stationary spots to the Ar^+ laser for 14 hours while collecting spectra every half hour.

3. Results

White light microscope images were collected for the waveguides written with the MHz laser. Two examples (side view) are shown in Figure 1. For scan speeds below 2 mm/s smooth lines were observed, whereas scan speeds above 2 mm/s yielded macroscopically rougher lines, with micron scale variations. These micron scale variations are substantially larger than the maximum pulse to pulse separation of 5 nm, and are similar to features observed by others with high pulse repetition rate writing [17].

All of the lines written with the MHz laser in this study matched those written with the highest cumulative dose in reference 18, and exhibited good, low-loss, single-mode optical guiding with a symmetric beam profile. For lines written with the kHz laser, such good waveguides were only obtained for laser pulse energies below 1 μJ. Lines written with the kHz laser at pulse energies greater than 1 μJ showed substantial damage, and tended to scatter light [19-20].

Raman and fluorescence spectra were collected for each line written with the MHz laser, and from one high power (5 μJ pulse energy) and one low power (0.5 μJ) line written using the kHz laser. This provides for comparisons within the data set and comparisons to our earlier spectroscopic data on lines written with the kHz laser [19,20]. A sample spectrum for a MHz waveguide, shown in Figure 2, exhibits a broad, low intensity fluorescence band centered around 650 nm. The inset shows part of the Raman spectra of which the peaks at 605 cm^{-1} and 800 cm^{-1} are of particular interest.

The areas under the fluorescence and Raman peaks were measured for each of the modified lines and unmodified glass. The areas of the Raman peaks were calculated using a straight line baseline from 570 to 645 cm^{-1} for the 605 cm^{-1} peak, and from 750 to 870 cm^{-1} for the 800 cm^{-1} peak. The ratio of the 605 cm^{-1} / 800 cm^{-1} peaks was then calculated as a measure of the 605 cm^{-1} peak's relative intensity. The relative intensity of the 605 cm^{-1} peak is a measure of the concentration of 3-membered rings in the silica network [21-22]. Figure 3a depicts the ratio of each line normalized to that of the unmodified glass. The area under the fluorescence curve from 555 to 800 nm was

calculated using a zero intensity baseline. Figure 3b depicts the peak area of each line, divided by the peak area of the unmodified glass. For the MHz laser system, the Raman peak ratios show an approximate 2-fold increase of the 605 cm^{-1} peak, but there is no definitive dependence on scan speed or pulse energy. The fluorescence results show that all of the modified lines have substantially more fluorescence (~2.5x) than the unmodified material. The fluorescence intensities for the kHz laser system are up to 3 orders of magnitude higher than those for the MHz laser system.

Additional fluorescence and Raman scans were performed across several of the waveguides written with the MHz laser to provide information on the spatial extent of the structural changes. The graphs presented in Figure 4 are the result of averaging 6 scans for each line. The data in Figure 4 is normalized to the signal from the unmodified glass. Both fluorescence and Raman spatial profiles have a FWHM of about 2.0 ± 0.5 microns. This is in good agreement with the linewidth obtained from the white light micrographs in Figure 1. The kHz lines (data not shown) show similar fluorescence and Raman waveguide profiles except that the lines are about 6 microns in diameter.

Fluorescence photobleaching studies were also conducted for waveguides formed by various laser writing conditions by using a low power (30 mW) Ar^+ laser to probe the fluorescence from fs-laser induced defects. During exposure to the low power Ar^+ beam the fluorescence intensity continuously decreased, as previously observed for lines written with the kHz laser system [20]. The photobleaching results are shown in Figure 5. Each graph shows the spectrum of the unmodified glass, the spectrum of the waveguide

region and the spectrum of the same region after prolonged exposure to the low power Ar^+ laser. Figure 5a shows that the fluorescence decreases by about two-thirds after 14 hours for the 115 nJ, 0.5 mm/s MHz waveguide. This is typical for all of the lines written with the MHz repetition rate, and was also seen for kHz repetition rate, but only above a 1 μJ pulse energy (Figure 5b). However, the kHz line has a far greater initial intensity indicating more defects were formed. The low pulse energy kHz line (Figure 5c) bleached completely within 14 hours of Ar^+ laser exposure, even though the initial fluorescence intensity was similar to that from waveguides formed by the MHz laser. The fluorescence peak of the low-intensity kHz line is centered at a wavelength less than 650 nm. Comparing the spectra in Figure 5c to similar 0.25 and 0.53 μJ data in Figure 5 of reference 20, the fluorescence peak is centered near 550 nm. Finally, it is worth noting that photobleaching of the fluorescence defects did not have a noticeable effect on the guiding characteristics of the waveguides.

4. Discussion

The 650 nm fluorescence band in all of the waveguides written with the megahertz fiber laser matches the non-bridging oxygen hole center (NBOHC) defect band that has been observed in higher power damage lines written with a kilohertz amplified laser [19,20]. However, it should be noted that the total fluorescence change in the MHz lines is a hundredth of that observed in the high pulse energy kHz lines. To understand the different material responses associated with different writing conditions in general it is important to determine which writing parameter (e.g. pulse fluence, peak

intensity, total exposure) controls defect formation and structural changes. In Table I fluorescence and Raman results for a number of representative writing conditions are analyzed in terms of a variety of laser parameters. The data in the Table clearly show that neither of the spectroscopic signals linearly scale with either pulse fluence, peak intensity or total dose. As expected, increasing the peak intensity causes a greater material change leading to more defects and greater fluorescence. Surprisingly, in the case of the MHz laser system increasing the total exposure leads to less fluorescence, indicating fewer defects.

We believe that the slight decrease in the fluorescence with increasing exposure in the MHz case is the result of thermal accumulation partially annealing the modified region while writing. The low thermal conduction in glasses prevents the absorbed laser energy from diffusing out of the focal region during the interval between pulses while writing with high repetition rate lasers. Partial annealing also explains why the fluorescence signal is substantially higher for kHz writing than for MHz writing. Other groups have reported large diameter modified regions forming in other glasses as a result of thermal accumulation [16-17]. A similar increase in diameter was not observed in our sample within the range of processing conditions studied (Figure 4) [25].

It can be demonstrated that a second type of fluorescent defect is present near 550 nm in the low pulse energy, kHz repetition rate case, shown in Figure 5c. This fluorescence band bleaches approximately 25% faster than NBOHC defects, matching characteristics associated with the $E_{\delta}^{'}$ defects from very small silicon nano-clusters that

several groups have reported seeing in γ-irradiated fused silica [26-27]. The absence of these defects in both higher energy kHz damage lines or MHz waveguides can again be accounted for by photobleaching while writing. Alternatively, for the high pulse energy kHz lines there is so much fluorescence from the NBOHC that it may overshadow the $E_{\delta}^{'}$ centers. Since these defects form at lower pulse energies than the NBOHC defects, the $E_{\delta}^{'}$ centers have a lower energy barrier for formation as well as for bleaching.

The waveguides written with both laser systems appear to retain good guiding behavior after Ar^{+} laser photobleaching of the NBOHC or $E_{\delta}^{'}$ defects. This indicates that the fluorescent defects are not responsible for the refractive index changes that result in guiding behavior. This is further supported by the observation that the waveguides written with the MHz system have a greater refractive index change despite having less fluorescence than the waveguides written with the kHz system.

The increase in the 605 cm^{-1} / 800 cm^{-1} Raman peak ratio observed for lines written with the MHz laser indicates an increase in the relative concentration of 3-membered rings. This behavior parallels the trend observed in lines written using the kHz laser. However, the absolute magnitude of the change is greater for the MHz lines than for the low pulse energy kHz line. The concentration of 3-membered rings observed in the high pulse energy kHz line is similar to the concentration observed in the MHz waveguides, but the kHz waveguide shows significantly more light scattering and does not exhibit good waveguiding. Since a greater concentration of 3-membered rings is associated with an increased local refractive index [19-22] our results support the

contention that in fused silica, high repetition rate modification yields good quality waveguides with a greater refractive index increase than low repetition rate modification [18].

5. Conclusion

Our results show that NBOHC defects are formed during waveguide fabrication with a 1 MHz fiber laser. Far fewer defects were formed with the MHz laser than with high pulse energy kHz writing. The fluorescent intensity in the MHz lines is similar to the fluorescence intensity of low pulse energy kHz lines, however, the nature of the defects formed are different. We also observed an increase in the relative intensity of the 605 cm^{-1} Raman peak, corresponding to an increase in the concentration of 3-membered rings in the lines fabricated with a MHz laser.

Acknowledgments

This work was performed under the auspices of the US Department of Energy by the University of California Lawrence Livermore National Laboratory, through M Division within Physics and Applied Technology, under contract W-7405-Eng-48, UCRL-JRNL-215987. The authors acknowledge financial support through National Science Foundation grant DMR - 0307002.

REFERENCES

[1] Davis KM,Miura K, Sugimoto N and Hirao K, “Writing waveguides in glass with a femtosecond laser,” *Opt. Lett.,* **21** 1729–31, (1996).

[2] Miura K, Qiu J R, Inouye H, Mitsuyu T and Hirao K, “Photowritten optical waveguides in various glasses with ultrashort pulse laser,” *Appl. Phys. Lett.,* **71** 3329–31, (1997).

[3] Hirao K and Miura K, “Writing waveguides and gratings in silica and related materials by a femtosecond laser,” *J. Non-Cryst. Solids,* **239** 91–5, (1998).

[4] Schaffer C B, Brodeur A, Garcia J F and Mazur E, “Micromachining bulk glass by use of femtosecond laser pulses with nanojoule energy,” *Opt. Lett.,* **26** 93–5, (2001).

[5] Homoelle D, Wielandy S, Gaeta A L, Borrelli N F and Smith C, “Infrared photosensitivity in silica glasses exposed to femtosecond laser pulses,” *Opt. Lett.,* **24** 1311–13, (1999).

[6] Efimov OM, Glebov L B, Richardson K A, Van Stryland E, Cardinal T, Park S H, CouziMand Bruneel J L, “Waveguide writing in chalcogenide glasses by a train of femtosecond laser pulses,” *Opt. Mater.,* **17** 379–86, (2001).

[7] Miura K, Jianrong Q, MitsuyuT and Hirao K, “Preparation and optical properties of fluoride glass waveguides induced by laser pulses,” *J. Non-Cryst. Solids,* **257** 212–19, (1999).

[8] Streltsov A M and Borrelli N F, "Fabrication and analysis of a directional coupler written in glass by nanojoule femtosecond laser pulses" *Optics Letters* **26**(1) 42-43, (2001).

[9] Sikorski Y, Said A A, Bado P, Maynard R, Florea C and Winick K A, "Optical waveguide amplifier in Nd-doped glass written with near-IR femtosecond laser pulses" *Electronics Letters* **36**(3) 226-227, (2000).

[10] Jones S C, Braunlich P, Casper R T, Shen X A and Kelly P, “Recent progress on laser-induced modifications and intrinsic bulk damage of wide-gap optical-materials,” *Opt. Eng.,* **28** 1039–68, (1989).

[11] Liu X, Du D and Mourou G, “Laser ablation and micromachining with ultrashort laser pulses,” *IEEE J. Quantum Electron.* **33,** 1706–16, (1997).

[12] Schaffer C B, Brodeur A and Mazur E, “Laser-induced breakdown and damage in bulk transparent materials induced by tightly focused femtosecond laser pulses,” *Meas. Sci. Technol.,* **12** 1784–94, (2001).

[13] Stuart B C, Feit MD, Herman S, Rubenchik A M, Shore BWand Perry MD, “Nanosecond-to-femtosecond laser-induced breakdown in dielectrics,” *Phys. Rev.* B, **53** 1749–61, (1996).

[14] Du D, Liu X, Korn G, Squier J and Mourou G, “Laser-induced breakdown by impact ionization in SiO2 with pulse widths from 7 ns to 150 fs,” *Appl. Phys. Lett.,* **64** 3071–3, (1994).

[15] Glezer E N and Mazur E, “Ultrafast-laser driven micro-explosions in transparent materials,” *Appl. Phys. Lett.,* **71** 882–4, (1997).

[16] Schaffer CB, Brodeur A, Garcia JF, Mazur E, “Micromachining bulk glass by use of femtosecond laser pulses with nanojoule energy,” *Opt. Lett*., **26** 93-95, (2001).

[17] Osellame R, Chiodo N, Maselli V, Yin A, Zavelani-Rossi M, Cerullo G, Laporta P, Aiello L, De Nicola S, Ferraro P, Finizio A, and Pierattini G, “Optical properties of

waveguides written by a 26 MHz stretched cavity Ti : sapphire femtosecond oscillator," *Opt. Expr.*, **13** 612-20, (2005).

[18] Shah L, Arai AY, Eaton S M, and Herman P R, "Waveguide writing in fused silica with a femtosecond fiber laser at 522 nm and 1 MHz repetition rate," Opt. Expr., **13** 1999-2006, (2005).

[19] Chan J W, Huser T, Risbud S and Krol D M, "Structural modification of vitreous silica after exposure to femtosecond laser pulses" *Opt. Lett.,* **26** 1726–8, (2001).

[20] Chan JW, Huser T R, Risbud S H and Krol D M "Modification of the fused silica glass network associated with waveguide fabrication using femtosecond laser pulses" *Appl. Phys.* A **76** 367–72, (2003).

[21] Geissberger A E, Galeener F L, "Raman studies of vitreous SiO_2 versus fictive temperature" *Phys. Rev.B.*, **28** 3266–71, (1983).

[22] Pasquarello A, Car R, "Identification of Raman defect lines as signatures of ring structures in vitreous silica," *Phys. Rev. Lett*., **80** 5145–7, (1998).

[23] Okuno M, Reynard B, Shimada Y, Syono Y, Willaime C, "A Raman spectroscopic study of shock-wave densification of vitreous silica," *Phys. Chem. Minerals* **26** 304–11, (1999).

[24] Kubota A, Caturla M J, Stolken J S, Feit M D, "Densification of fused silica due to shock waves and its implications for 351 nm laser induced damage," *Opt. Expr.*, **8** 611–16, (2001).

[25] Eaton S M., Zhang H, Herman P R., Yoshino F, Shah L, Bovatsek J, Arai A Y, "Heat accumulation effects in femtosecond laser written waveguides with variable repetition rate," Opt. Expr., **13** 4708-4716, (2005).

[26] Nishikawa H, Watanabe E, Ito D, Sakurai Y, Nagasawa K, Ohki Y, "Visible photoluminescence from Si clusters in γ-irradiated amorphous SiO_2," *J. Appl. Phys.* **80** 3513-3519, (1996).

[27] Demos S, Staggs M, Minoshima K, Fujimoto J, "Characterization of laser induced damage sites in optical components," *Opt. Expr.*, **10** 1444-1450, (2002).

Table I. Comparison of laser modification with MHz and kHz lasers.

Writing conditions							**Spectroscopy**	
Pulse energy E (μJ)	Spot size[a)] A (μm^2)	Rep rate r (s^{-1})	Scan speed[b)] v (mm/s)	**Pulse fluence F (J/cm^2)**	**Peak intensity[c)] I (TW/cm^2)**	**Total dose[d)], D (MJ/cm^3)**	**Fluor. signal (a.u)**	**Raman signal (a.u)**
0.115	0.27	10^6	0.05 T	**43**	**85**	**8500**	**5.4**	**2.7**
0.115	0.27	10^6	5 T	**43**	**85**	**85**	**6.5**	**2.5**
0.3	1.51	10^3	0.02 T	**20**	**150**	**5**	**4.1**	**1.0**
5.0	1.51	10^3	0.02 T	**330**	**2500**	**88**	**1300**	**1.5**
0.5	1.51	10^3	0.02 L	**33**	**250**	**16**	**170**	**1.1**
5.0	1.51	10^3	0.02 L	**330**	**2500**	**160**	**1000**	**1.9**

[a)] The spot size A was calculated as $A = \pi w_0^2$; w_o (the spot radius) = $M^2\lambda/(\pi NA)$, where $M^2 = 1.5$ is the beam quality factor, λ is the laser wavelength, and NA is the numerical aperture of the focusing objective.
[b)]The T/L symbol refers to a transverse/longitudinal writing geometry.
[c)] The pulse intensity was calculated as $I = F/\tau$; for the kHz laser the pulse duration, τ, is 130 fs. For the MHz laser the pulse duration is less accurately known, an upper limit of 500 fs was used in our calculations.
[d)] For the case of longitudinal writing (last two rows) the total dose, $D = Fr/v$; for the case of transverse writing (first four rows) $D = Fr(NA)/v$.

Figure Captions

1. White light images of lines written with the MHz system using a pulse energy of 115 nJ, and scanning the sample transversely at a) 0.05 mm/s and b) 5 mm/s. The circular fringes are artifacts from the microscope. Dashed lines indicate the approximate boundary of the waveguides.

2. Sample spectrum of a waveguide written with the MHz laser system using a laser pulse energy of 115nJ, and scanning the sample transversely at 0.5 mm/s.

3. a) Normalized 605 cm^{-1} / 800 cm^{-1} Raman peak ratios and b) fluorescence intensities for lines written using a 1 MHz repetition rate laser system at different scan speeds and pulse energies. The data is normalized with respect to the unmodified glass.

4. a) 605 cm^{-1} / 800 cm^{-1} Raman peak ratio, and b) fluorescence intensity spatial profile for waveguides written with a 1 MHz laser and 115nJ pulse energy. Both plots are normalized to the data for unmodified glass.

5. Fluorescence of fs-laser modified lines after 14 hours of exposure to 30 mW of Ar^+ laser light. The initial fs laser modification conditions were a) 1 MHz repetition rate, 115nJ pulse energy, 0.5 mm/s scan speed b) 1 kHz, 5 μJ, 20 μm/s c) 1 kHz, 0.5 μJ, 20 μm/s. All spectra were recorded with a 5 minute acquisition time.

Figure 1.

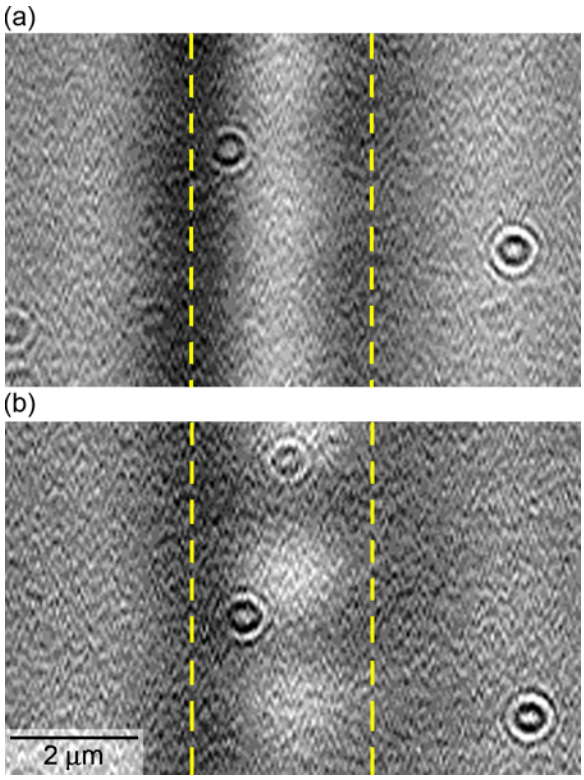

Figure 2.

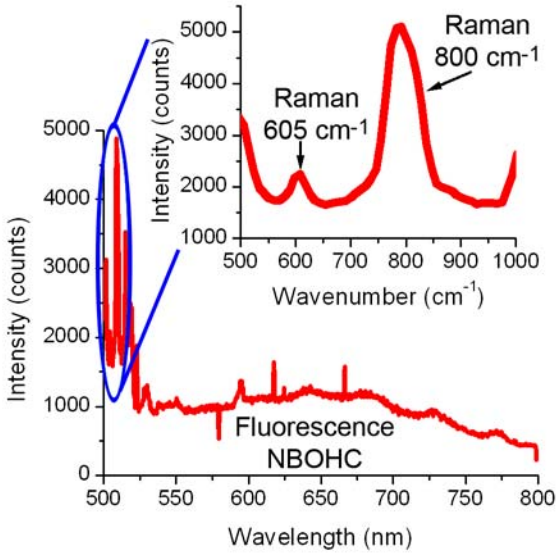
Raman
800 cm-1
Raman
605 cm-1
Intensity (counts)
Wavenumber (cm-1)
Fluorescence
NBOHC
Intensity (counts)
Wavelength (nm)

Figure 3.

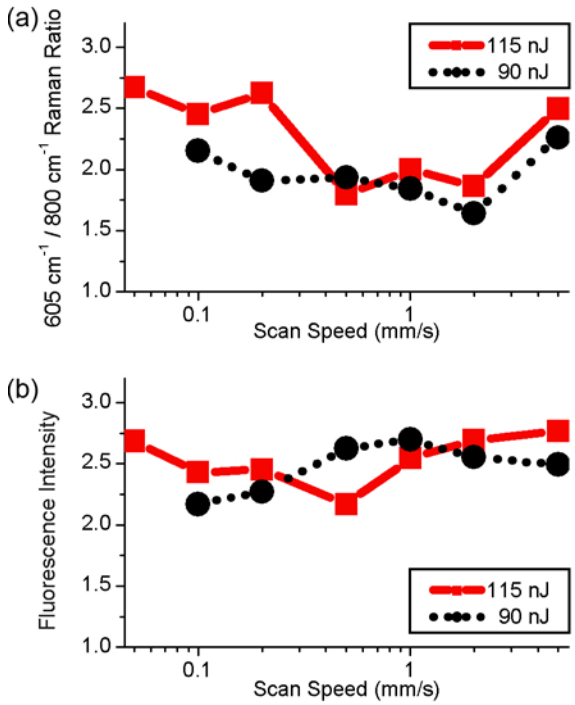
(a)
605 cm-1 / 800 cm-1 Raman Ratio
3.0
2.5
2.0
1.5
1.0
0.1
1
Scan Speed (mm/s)
115 nJ
90 nJ
(b)
Fluorescence Intensity
3.0
2.5
2.0
1.5
1.0
0.1
1
Scan Speed (mm/s)
115 nJ
90 nJ

Figure 4.

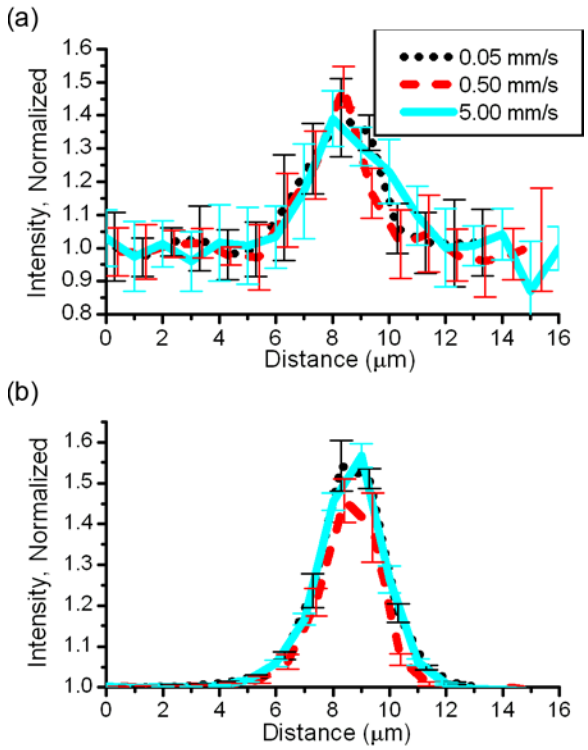
(a)
0.05 mm/s
0.50 mm/s
5.00 mm/s
Intensity, Normalized
Distance (μm)
(b)
Intensity, Normalized
Distance (μm)

Figure 5.

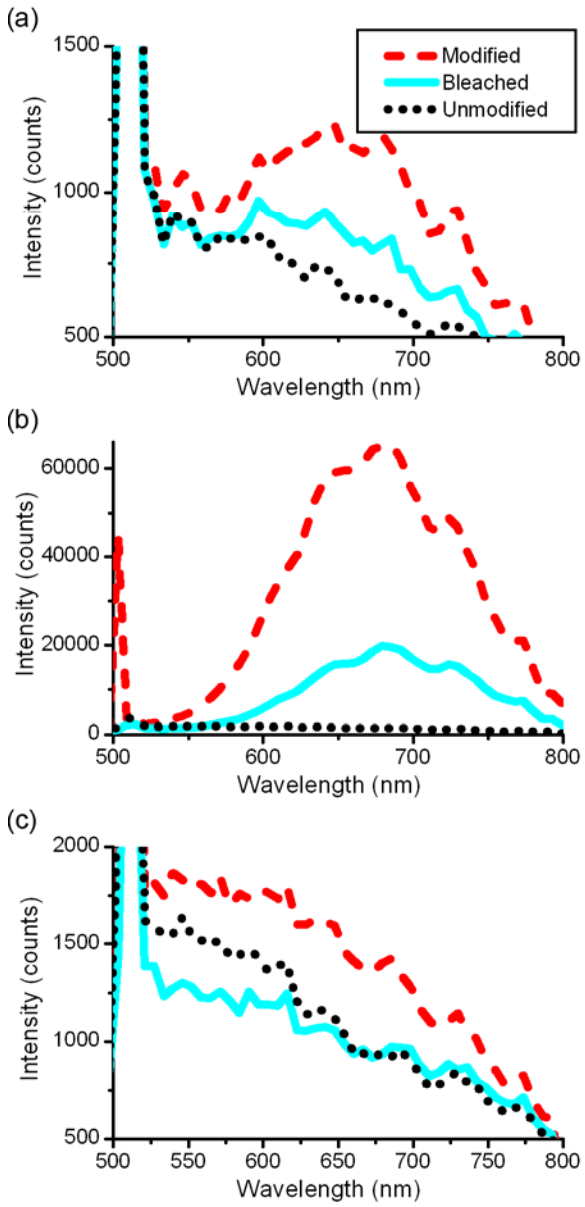
(a)
Modified
Bleached
Unmodified
Intensity (counts)
1500
1000
500
500
600
700
800
Wavelength (nm)
(b)
Intensity (counts)
60000
40000
20000
0
500
600
700
800
Wavelength (nm)
(c)
Intensity (counts)
2000
1500
1000
500
500
550
600
650
700
750
800
Wavelength (nm)